sustainability

MDPI

Article

Integrating Geosynthetics and Vegetation for Sustainable Erosion Control Applications †

Tatiana Olinic [1,*], Ernest-Daniel Olinic [2,*] and Ana-Cornelia Butcaru [3]

[1] Faculty of Land Reclamation and Environmental Engineering, University of Agronomic Sciences and Veterinary Medicine Bucharest, 011464 Bucharest, Romania
[2] Faculty of Hydrotechnics, Technical University of Civil Engineering Bucharest, 020396 Bucharest, Romania
[3] Research Center for Studies of Food Quality and Agricultural Products, University of Agronomic Sciences and Veterinary Medicine Bucharest, 011464 Bucharest, Romania; ana.butcaru@qlab.usamv.ro
* Correspondence: tatiana.olinic@fifim.ro (T.O.); ernest.olinic@utcb.ro (E.-D.O.)
† This article is a revised and expanded version of papers entitled [The role of geosynthetic materials and vegetation on slope erosional control: Results of scale model tests], which was presented at [the 5th Pan-American Conference on Geosynthetics, Toronto, ON, Canada, 28 April–1 May 2024]; and [The effect of living plant roots on the shear strength parameters: A sustainable approach to shallow slope stability and erosion control applications], which was presented at [the 4th International Conference on Sustainable Development in Civil, Urban and Transportation Engineering, Wroclaw, Poland, 14 October 2024].

Abstract: The stability of slopes is a critical challenge in various civil engineering projects, such as embankments, cut-slopes, landfills, dams, transportation infrastructure, and riverbank restoration. Stabilizing slopes using bioengineering methods is a sustainable approach that limits the negative impact of engineering works; such methods should be implemented and adopted worldwide. Geosynthetic materials and plant roots are sustainable for preventing erosion and surface landslides. The plants used for this paper are known to have beneficial effects on erosion control, namely *Festuca arundinaceous*, *Dactylis glomerata*, *Phleum pratensis*, *Trifolium pratense*, and *Trifolium repens*. Using vegetation as a bio-reinforcement method is often more cost effective and environmentally friendly than traditional engineering solutions, making a more sustainable engineering solution for shallow slope stabilization applications. The paper presents the erosion process that occurred on sandy slopes protected by organic soil layers and geosynthetic materials under rainfall simulation in scaled model tests.

Keywords: roots reinforcement; direct shear test; soil bioengineering; erosion control; geosynthetics

check for updates

Citation: Olinic, T.; Olinic, E.-D.; Butcaru, A.-C. Integrating Geosynthetics and Vegetation for Sustainable Erosion Control Applications. *Sustainability* **2024**, *16*, 10621. https://doi.org/10.3390/su162310621

Academic Editor: Lucio Di Matteo

Received: 28 October 2024
Revised: 27 November 2024
Accepted: 29 November 2024
Published: 4 December 2024

Copyright: © 2024 by the authors. Licensee MDPI, Basel, Switzerland. This article is an open access article distributed under the terms and conditions of the Creative Commons Attribution (CC BY) license (https://creativecommons.org/licenses/by/4.0/).

1. Introduction

The stability of slopes is a critical challenge in various civil engineering projects, such as embankments [1], cut-slopes, landfills, dams, transportation infrastructure [2], and riverbank restoration [1,3]. Geosynthetic materials for erosion control have demonstrated their effectiveness in improving shallow slope stability. These materials can reinforce the topsoil, increasing its shear strength and reducing the risk of shallow slope failures. Alongside the use of geosynthetics for erosion control, the use of vegetation in slope stabilization systems has gained increasing attention. Through their extensive root systems, living plants can stabilize shallow slopes [4] and offer sustainable, long-term solutions.

Ecological slope protection not only has the function of traditional slope protection, but it also integrates various aspects such as landscape, culture, and ecology, thereby achieving the maintenance and restoration of natural ecosystems [5]. The roots of plants developed on the entire slope generate both hydrological and mechanical effects, contributing to erosion protection and slope stabilization of the complex as a whole [6]. Also, it is considered that this practice is strongly dominated by empiricism [3].

Tension-bearing plant roots infiltrate soil pores, enhancing the shear strength of the soil-root matrix. In past decades, mechanical root reinforcement has been extensively

quantified experimentally and analytically, and this effect is usually included in slope stability calculations [7].

In civil and environmental engineering projects, geosynthetic materials for erosion control are often essential during construction to mitigate soil loss and prevent sediment runoff in the short and long term to support the growth and maintenance of dense vegetation. This vegetation, after a period, protects slopes from splash and sheet erosion, thereby effectively preventing the formation of rill erosion [8].

The life cycle cost analysis (LCCA) of geosynthetics evaluates the total expenses of these materials over their lifespan in erosion control projects. It considers initial costs (purchase, transport, and installation), maintenance or repair expenses during use, and disposal costs at the project's end. This comprehensive assessment helps to identify cost-effective solutions, highlighting geosynthetics' long-term financial benefits. These materials often reduce maintenance needs and enhance durability, making them a sustainable choice. Ultimately, geosynthetics offer significant savings over their life cycle compared to alternative methods.

Water-induced erosion degrades soil quality, leading to reduced crop yields. Understanding how crop yields respond to soil erosion is crucial for evaluating agriculture's susceptibility to such degradation. Research conducted in [9] suggests that quantifying the reduction in crop yields due to erosion is a challenging topic. Soil erosion occurs when topsoil is displaced by natural forces such as wind and water [10]. The erosion process increases with greater soil exposure, especially during rain or windstorms. When topsoil is lost, the soil's most nutrient-dense layer is removed, leading to a decline in overall soil quality.

Additionally, many studies investigate how soil erosion affects soil and plant properties, as well as its impact on associated ecosystem services. Research conducted in [11] emphasized that soil erosion has profound consequences on the functioning of ecosystems and the services they provide. The authors recommended soil conservation and ecosystem restoration measures to prevent further degradation and to protect soil, biodiversity, and agricultural productivity. Turcu et al. (2024) point out that plowing in hilly areas can affect soil surface roughness, altering flow rate, water infiltration time, and infiltration and runoff processes [12].

Vegetation influences slope stability and erosion through mechanical support and hydrological effects. Yen (cited by Cazzuffi et al., 2014) categorized roots into five classes, identifying H-type and VH-type roots as optimal for stabilization and wind resistance [13]. Mairaing et al. (2024) studied plants in Thailand's highlands, noting their strong anchoring roots and lateral systems that reduce water-induced erosion. The study recommended using robust-rooted plants for effective slope stabilization and erosion control [14].

The presence of roots can modify the soil's hydrological behavior by increasing soil suction, which helps to retain water and reduces pore water pressure, thereby enhancing the overall stability of slopes. Research conducted by Lobmann et al. has shown that the tensile strength of roots contributes directly to the slope's resistance against gravitational forces, particularly under wet conditions [15]. As highlighted by Cao et al., plant roots not only reinforce the soil mechanically but also regulate the soil moisture content by enhancing water infiltration and reducing surface runoff. Their research demonstrates that root systems contribute to maintaining slope stability by balancing soil moisture levels, especially during heavy rainfall events. This protective mechanism is crucial for preventing slope failures, further supporting the role of vegetation in slope stabilization efforts [16].

Under seismic or cyclic loading, the arrangement and interaction of sand particles are critical in resisting liquefaction, as shown in discrete element method (DEM) studies. Plant roots enhance soil stability by increasing particle contact, reducing void spaces, and improving resistance to dynamic stresses [4,16]. Zhao et al. demonstrated that while roots may not prevent liquefaction outright, they reinforce sandy soils by stabilizing particle arrangements during loading. This reinforcement reduces deformation and increases the

soil's liquefaction threshold compared to bare soils. Rooted soils thus exhibit greater stability under dynamic conditions, mitigating rapid strength loss [17].

Engineering judgment involves using various methods, including horizontal drains, slope reinforcement techniques, soil hardening measures, surface water management techniques, groundwater control methods, and proper vegetation management [18], to prevent slope failure under rainfall conditions.

The aim of this study is structured around three distinct stages, utilizing different experimental setups, namely: plant selection and root development, improvement of the shear strength parameters by plant roots, and the study of the impact of heavy rainfall on erosion and slope stability.

The first stage involved selecting plant species that naturally live in a temperate continental climate. The growth of these plants' root systems was studied in different types of soil, including various thicknesses of organic soil, as well as in sand-based fill material.

The second stage focused on determining the shear strength parameters of sand, organic soil, and at the sand–organic soil interface, both with and without the presence of plant roots.

The third stage examined the effect of heavy rainfall on erosion and the stability of a scaled model embankment. The critical moments that appeared during heavy rainfall tests included: after the sand excavation was completed (prior to applying the organic soil), after the organic soil layer was added, post-germination of plants (immature vegetation), after installing geosynthetic materials, once the plants reached full maturity, and after plant desiccation.

This study builds upon existing research conducted on scaled models, with significant differences in key areas such as: vegetation growth (unlike many studies where vegetation was grown horizontally and slopes were inclined during testing, our research involved natural growth directly on the inclined model slope), controlled rainfall simulation (rainfall was simulated in a controlled and uniform manner), and exposure to natural environmental conditions (the scaled model tests were exposed to natural variations in humidity and temperature, including winter freezing and summer desiccation).

Stabilizing slopes using bioengineering methods is a sustainable approach that limits the negative impact of engineering works; such methods should be implemented and adopted worldwide.

2. Materials and Methods

2.1. Used Materials

2.1.1. Geosynthetics for Erosion Control—Geomats

From a design perspective, using geosynthetics in engineering applications now represents a sustainable and well-established technological solution. Geosynthetics, durable construction materials used in engineering, exemplify a successful approach to sustainable development [19].

Geomats—three-dimensional geosynthetic materials—are widely used to prevent soil erosion caused by wind or water. These porous structures are placed on slope surfaces and are particularly effective on steep slopes, providing stability for plant roots, encouraging vegetation growth, and strengthening erosion resistance [20,21]. These erosion control systems may be required in civil and environmental engineering projects as a short-term solution during construction to limit soil loss and sediment runoff from the site and as a long-term solution to establish dense vegetation coverage that protects slopes from splash and sheet erosion while preventing rill erosion [8].

Geosynthetics provide an affordable, long-lasting, and eco-friendly approach to soil erosion control and slope stabilization in diverse civil engineering projects [22]. Their capacity to blend with natural environments and their mechanical solid properties render them essential in contemporary erosion control methods.

The geosynthetic materials used for erosion control in this study consisted of two HDPE (high-density polyethylene) and PP (polypropylene) geomatics (named GEC1 and GEC2,

respectively) and one geo-blanket made from biodegradable materials (Jute, named GEC3) (Figure 1). These materials were provided strictly for this study by two manufacturing and supply companies of geosynthetic materials.

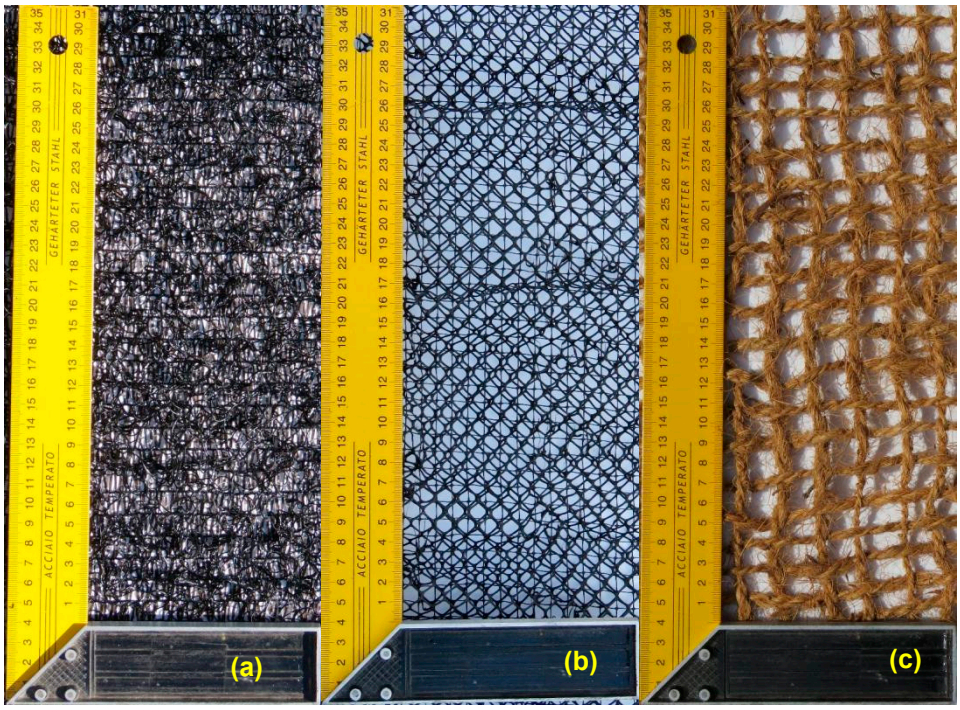

Figure 1. The geosynthetic materials used for this study: (**a**) GEC 1, (**b**) GEC 2, and (**c**) GEC 3.

GEC1 is a PP-based, three-dimensional synthetic erosion control solution designed to permanently reinforce the grass-root matrix, providing long-term surface erosion protection. This product is ideal for applications where vegetation needs continuous support to shield the soil from weather and water erosion. Its densely interwoven strands mimic the function of a root system, binding soil particles and bonding fertile humus to strengthen the soil structure. The mechanical properties are tensile strengths in the length direction of 1.3 kN/m and in the cross direction of 0.5 kN/m; the strain at maximum strength in both directions is 50% (± 25%). The physical properties are a melting point of 150 °C, mass per unit area of 350 g/m^2 (±40), PP single filament diameter of 500 µm (±30%), void index above 90%, and thickness at 2 kPa of 18 mm (±2 mm).

GEC2 comprises three layers: a rhombic HDPE net as the base layer, a bi-oriented PP reinforcement layer in the middle, and another HDPE net that gives the product its wave-like shape and thickness. This material is designed to support vegetation growth and provide erosion control on slopes and channels, utilizing its volumetric structure. The wave-shaped design helps to trap newly laid soil and seeds. The mechanical properties provided are a tensile strength of 3.5 kN/m at 20% elongation. The physical properties are a mass per unit area of 340 g/m^2 (±40) and 20 to 25 mm thickness.

The GEC3 jute fiber fabric is designed for temporary use, effectively reducing soil erosion from heavy rainfall, supporting initial vegetation growth, and serving as interception storage. Made from renewable and biodegradable jute fibers, the product consists of double-twisted jute woven in the warp (longitudinal) and weft (transverse) directions using a plain weave. Its variable and flexible mesh structure is ideal for promoting plant growth. The percentage of threads shading of approx. 50% and thread thickness of approx. 2.65 mm provides a balance between erosion protection and greening potential. With its high water absorption capacity, the fabric minimizes erosion while acting as a moisture reservoir, gradually releasing water from the jute fibers. This material has a tensile strength of 5 to 7.5 kN/m and a mesh spacing from wrap-to-wrap × weft-to-weft of 20 × 30 mm.

Geosynthetic materials for erosion control promote vegetation growth and increase the long-term resistance of grass cover to a higher duration flow velocity. Since the grass is well developed, the slope is naturally reinforced by roots and the longevity and durability costs are zero. GEC3 is a biodegradable blanket that provides soil erosion protection and permits vegetation to grow on moderate slopes, while GEC1 and GEC2 are degradable products; therefore, for all these materials, the end-of-life costs are zero in terms of LCCA.

2.1.2. Properties of Used Soils

The organic soil (OS) used in this study was a natural product commonly used for gardening, with an organic matter content ranging between 60 and 80% and a pH value of 5 to 7. The geotechnical characteristics of the OS are an internal friction angle of 19.57° and cohesion of 36.11 kPa. The soil used in all the tests is known as very erodible soil—sandy soil. From the granulometric perspective, it is a medium to coarse sand with poor gradation, according to SR EN ISO 14688:2-2018 [23] (Figure 2). The geotechnical characteristics of the bare sand (BS) are a specific gravity of 2.65 g/cm^3, internal friction angle of 32.94°, and cohesion of 1.24 kPa.

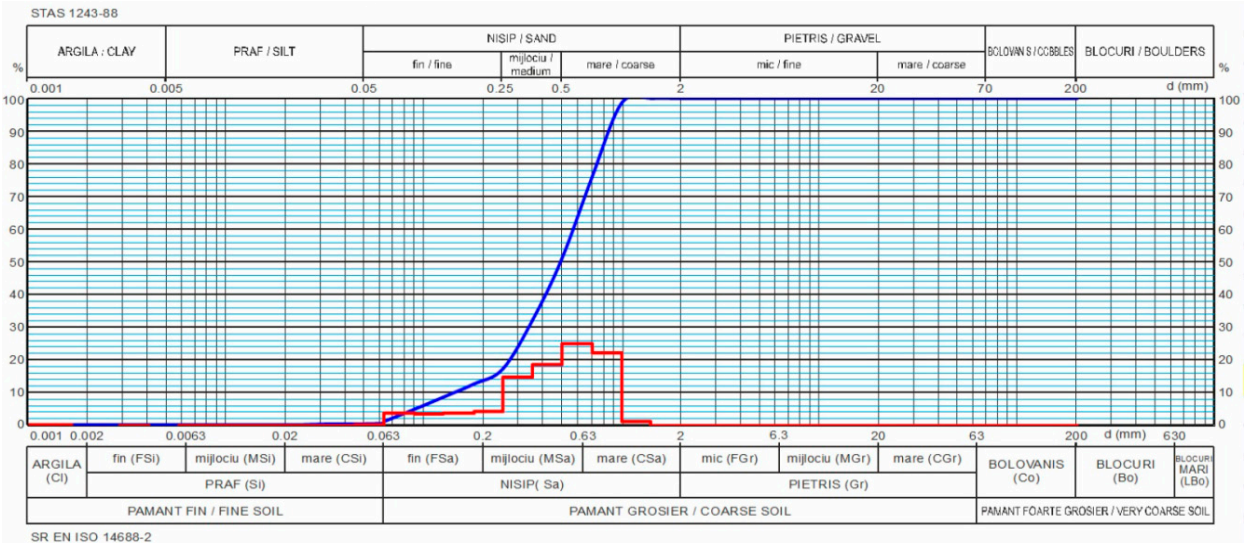

Figure 2. Grain size distribution (blue line) and the histogram (red line) of the sand sample.

2.1.3. Vegetation

The plants used for this paper are known to have beneficial effects in erosion control, namely *Festuca arundinaceous*, *Dactylis glomerata*, *Phleum pratensis*, *Trifolium pratense*, and *Trifolium repens.* Two seed mixtures were studied for the stage aimed at determining the optimal thickness of the topsoil layer for plant roots: Mix 1 and Mix 2. The plant mixture used in Mix 1 is recommended for use on artificial slopes according to the Design Guide GE 027-1997. This mixture has the following composition: *Dactylis glomerata* 40%, *Festuca arundinaceous* 30%, and *Trifolium pratense* 30%. Mix 2 is commonly used in grassland areas in Romania, specifically: *Festuca arundinaceous* 25%, *Dactylis glomerata* 25%, *Phleum pratensis* 20%, *Trifolium pratense* 10%, and *Trifolium repens* 20%. The seeds used in the research were sourced from a forestry research center, and all of the seeds are well known for being used for grassland.

2.2. Testing Methodology

To observe and quantify the beneficial effect of plant roots and geosynthetic materials on the stability and geometry of slopes, the following parameters were determined: the optimal thickness of the soil layer for root development, the characteristics and shape of the roots, the shear strength parameters of control samples and root samples taken from various

depths, the design of a scaled experimental model to observe the erosion phenomenon, as well as the design and calibration of a torrential rainfall simulator.

2.2.1. Optimum Organic Soil Thickness

To determine the optimal thickness of the OS layer for proper root development, seeds were sown in cylindrical containers filled with different amounts of sand and OS. The cylindrical containers, with a height of 27 cm and a diameter of 8 cm, were filled with layers of 5, 10, 15, and 20 cm of sand and 0, 5, 10, 15, and 20 cm of OS (Figure 3). Seeds from Mix 1 and Mix 2 were sown (on 30 September 2022) in single amounts (40 g/m^2) and double amounts (80 g/m^2), resulting in a total of 20 containers. The containers were placed in the University of Agronomic Sciences and Veterinary Medicine greenhouse in Bucharest at a constant temperature of 24 °C and controlled light and humidity throughout the autumn and winter.

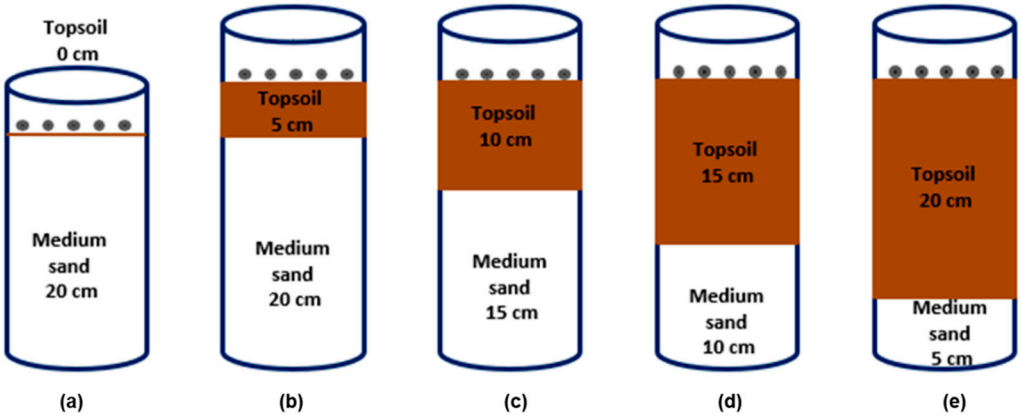

Figure 3. The distribution of the topsoil layer in the cylindrical containers to determine the optimum OS thickness: (**a**) 0 cm OS, (**b**) 5 cm OS, (**c**) 10 cm OS, (**d**) 15 cm OS, and (**e**) 20 cm OS.

For this activity, visual observations were made regarding plant germination, stem and leaf development, and root growth.

2.2.2. Scanning of Roots with WinRHIZO

The WinRHIZO system was used to assess root development in different variants. Leguminous (L) and Gramineae (G) plants were used in a mixed composition of *Festuca arundinacea* (25%), *Dactylis glomerata* (25%), *Phleum pratense* (20%), *Trifolium pratense* (10%), and *Trifolium repens* (20%), grown in OS layers with thicknesses of 0, 5, 10, and 20 cm (named L0–G0, L5–G5, L10–G10, and L20–G20, respectively).

WinRHIZO, created by Regent Instruments Canada Inc., Québec City, QC, Canada, includes an Epson 11000XL scanner and WinRHIZO Pro 2010b software for image processing [24]. It is a high-performance system that enables morphological measurements of the root system and analyzes a series of essential parameters, including root system length (cm), root system projection (cm^2), root surface area (cm^2), root volume (cm^3), average root diameter (mm), root classes according to scanned diameter, and roots apical tips.

The roots of each sample were washed with tap water to remove soil. They were then manually measured for length using a linear meter, placed into a 100 mL plastic tube, and submerged in water for volume measurement.

The roots of each sample were then scanned using WinRHIZO root-scanning equipment and WinRHIZO Pro 2010b software, allowing root length and volume to be measured from the scanned images. In the present study, we compared the size and root volume measured by the software with those determined manually.

2.2.3. Shear Test Strength

The direct shear test was carried out using the Shearmatic automatic direct/residual shear machine with programmable pneumatic loading produced by Wykeham Farrance (Cheshire, UK). According to geotechnical test method standard SR EN ISO 17892-10:2019 [25], the shear strength parameters were determined in unconsolidated, undrained, saturated conditions (UUsat) performed on initially saturated samples, with a shearing speed of 1.00 mm/min (Figure 4). The UUsat tests of the root-soil complex were conducted under various vertical pressures (25 kPa, 50 kPa, and 75 kPa) after a growth period of 150 days.

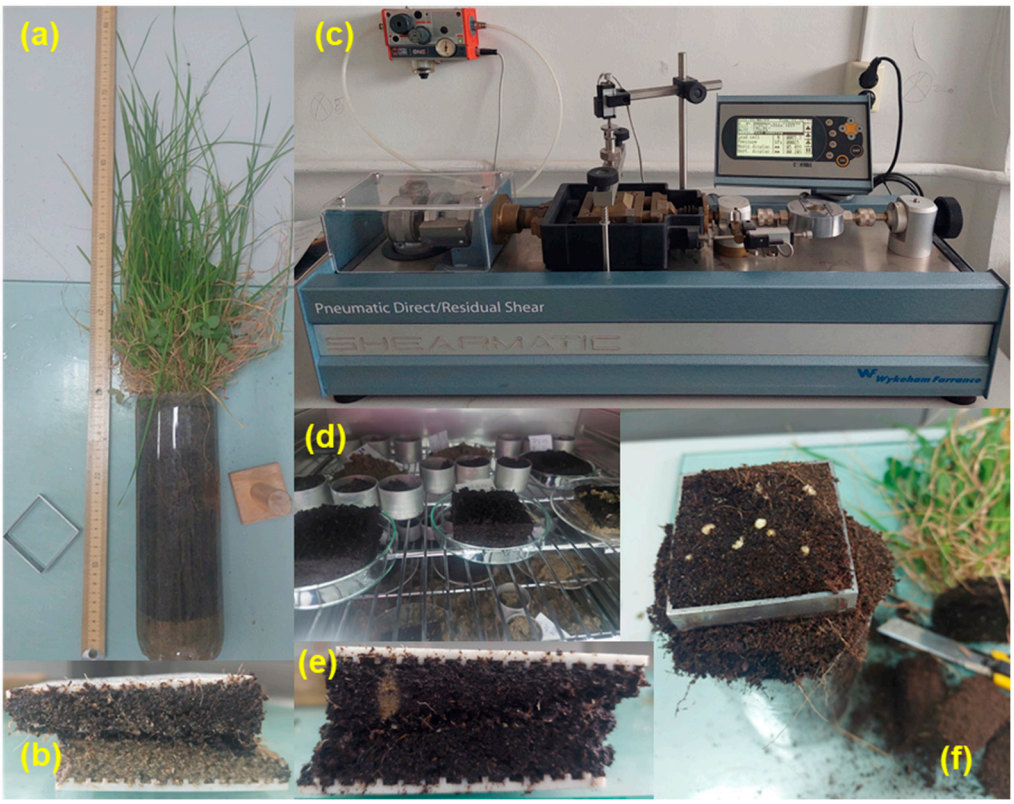

Figure 4. The direct shear methodology: (**a**) the sample of 20 cm OS with living vegetation, (**b**) sheared sample at the interface between OS and sand with roots, (**c**) the Shearmatic automatic direct/residual shear machine, (**d**) sheared samples in the oven, (**e**) sample of OS with roots sheared, and (**f**) sample taken from the upper part of the cylinder.

The Mohr–Coulomb failure criterion suggests that material failure occurs due to the combined effects of normal stress (σ_n) and shear stress (τ). In the context of a soil-root composite, the presence of roots can influence the overall shear strength of the soil, effectively increasing its resistance to failure. The criterion is represented mathematically by the Mohr–Coulomb equation:

$$\tau_f = c' + (\sigma_n - u) \times tan\varphi' + c_r, (\text{kPa}) \quad (1)$$

where τ_f is the shear strength (kPa), c' is the cohesion force, σ_n is the vertical stress (kPa), u is the total pore water pressure (kPa), φ' is the internal friction angle (°), and c_r is the cohesion force added by roots (kPa), often termed root-induced cohesion or pseudo-cohesion.

The term $(\sigma_n - u)$ represents the effective normal stress, which is the actual stress exerted on the soil particles after accounting for the pressure from the pore water. Including c_r reflects the roots' contribution to the soil's overall cohesion.

Direct shear tests were conducted on samples collected in the horizontal plane, with naturally developed roots oriented vertically. The failure plane intersected the roots trans-

versely, resulting in the maximum shear strength of the root-reinforced soil. If the samples would had been sheared along a plane parallel to the root growth direction, it is estimated that the shear strength parameters would have been significantly lower. Thus, the analysis accounted for the anisotropy of the root-reinforced soil.

2.2.4. Scale Model Devices: Erosion Control Chamber and Rainfall Simulator

The study observed erosion phenomena caused by torrential rainfall in a scaled model. The scaled model device consisted of two main components: (1) an erosion simulation chamber and (2) a rainfall simulator, both constructed from plexiglass (Figure 5).

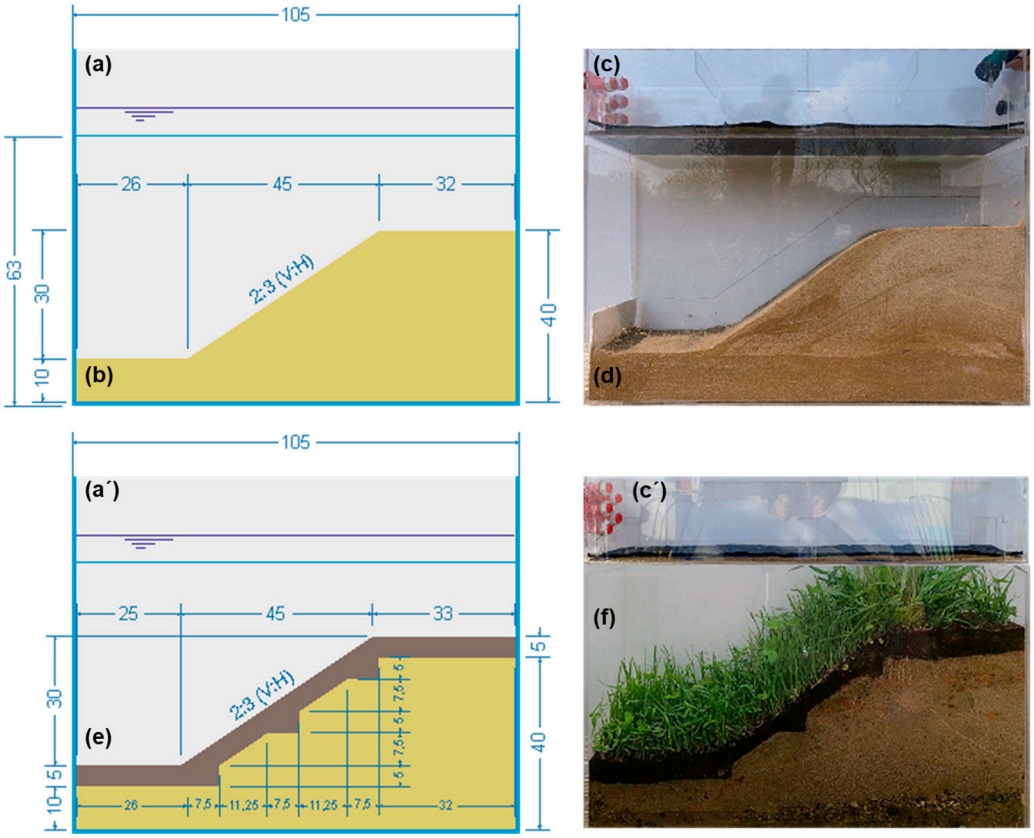

Figure 5. Scaled model device [26]: (**a**,**a'**) sketch of the rainfall simulator at the upper part, (**b**) sketch of the erosion control chamber with a slope of 2:3 (V:H), (**c**,**c'**) image of the rainfall simulator at the upper part, (**d**) image of the erosion control chamber with an artificial slope of 2:3 (V:H) realized by compacted sand (**e**) sketch of the erosion control chamber with the dimensions of the artificial slope protected by a 5 cm OS layer placed in steps, and (**f**) image of the erosion control chamber with an artificial slope protected by OS and mature vegetation.

These devices/boxes developed to simulate slope erosion were designed to meet several technical, economic, and practical requirements, including: (1) constructing the model at the smallest possible scale while still accurately representing the erosion phenomenon, (2) enabling measurements that effectively capture the magnitude and dynamics of the process, (3) closely replicating the effects of torrential rainfall, (4) demonstrating the role of geosynthetic materials in erosion control, (5) assessing the utility of a topsoil layer, (6) evaluating the thickness of this layer, and accounting for the (7) presence, (8) type, and (9) age of vegetation.

Six transparent plexiglass boxes, each measuring 105 cm in length, 63 cm in height, and 20 cm in thickness, were constructed for the erosion simulation chamber. The testing boxes were open-topped and designed to be in direct contact with the atmosphere while also allowing the attachment of the rainfall simulator. To ensure the boxes could support

the lateral pressure developed by the soil, a plexiglass sheet thickness of 1 cm was chosen, and one metal bar was installed to maintain a constant thickness of 20 cm.

These experimental boxes were placed in an experimental plot in Chiajna, Ilfov County, Romania. From May to September 2023, they were exposed to natural climatic conditions of humidity and temperature, with the exception of the first two weeks after planting when they were irrigated to facilitate germination and plant growth.

All experiments were recorded on video using a GoPro Hero 9, allowing observation of the dynamics of the slope erosion process and the changes in the slope profile due to the transport of displaced material from the upper to the lower part of the slope.

In the experimental boxes, artificial slopes with a 2:3 (V:H) gradient were created using very erodible soil with poorly graded medium sand. The sand was placed into the box in layers and lightly compacted by hand. Some tests were also conducted using topsoil layered onto the slopes in steps to create a bond between the two soil types. In trial tests where geosynthetic materials were used, the geomats were placed both on the slope and the horizontal surfaces. They were secured in the soil with two metal clamps, which were removed as the vegetation grew and the plants developed their root systems.

The study tracked erosion through visual observation, utilizing images taken throughout the the scale model tests. The extent of erosion was measured by calculating the volume of soil or other material that had been eroded, moved from its original location, and then accumulated at the base of the slope. This approach allowed for a detailed assessment of how much material was displaced during erosion events and where it was deposed.

Due to the nature of the experimental boxes and the inherent characteristics of the sandy slope, specific tests to determine the moisture content were not conducted. Hydraulic conductivity and air conductivity play significant roles regarding the time of soil saturation (organic soil and sandy soil in our tests). The experimental design focused on replicating the in situ conditions as closely as possible, which included the natural variability of moisture content in the sampled material, which became fully saturated after a certain amount of time. The saturation occurred relatively quickly in the test performed on sandy soils and a little bit later for the topsoil.

The rainfall simulator was a parallelepiped box with the exact base dimensions of the erosion simulation chamber (105 × 20 cm) and a height of 20 cm. Its base was perforated with 1 mm diameter holes arranged in a square grid with one cm^2 spacing. It served as a water reservoir with a perforated base, maintaining the water height at different levels to simulate varying rain intensities. The tests carried out in the experimental device consisted of simulating the effect of rain of 400 L/s, ha (144 mm/h) on a slope with a slope of 2:3 (V:H) and a height of 30 cm [26].

2.3. Climatic Conditions

The temperature and precipitation regimes influence most plant processes, including photosynthesis, transpiration, respiration, germination, and flowering. If the temperature exceeds a certain threshold, heat stress occurs in plants. To analyze this, meteorological data were collected from a nearby weather station from 1 May 2023 to 1 September 2023, specifically Weather Station ID: ICHIAJNA5, Latitude/Longitude: 44.459° N, 25.978° E.

An analysis of the meteorological data (Figure 6, based on meteorological data from Weather Station ID: ICHIAJNA5) revealed that there were 78 days during the analyzed period with temperatures exceeding 30 °C, meaning that heat stress was experienced during 63.93% of the period when plants were developing. Regarding precipitation, it was observed that over 122 days, the total rainfall was approximately 60 mm, which was insufficient for plant growth and maintenance. According to the National Meteorological Agency, 2023 was declared the hottest year since 1900 and considered one of the driest years since then.

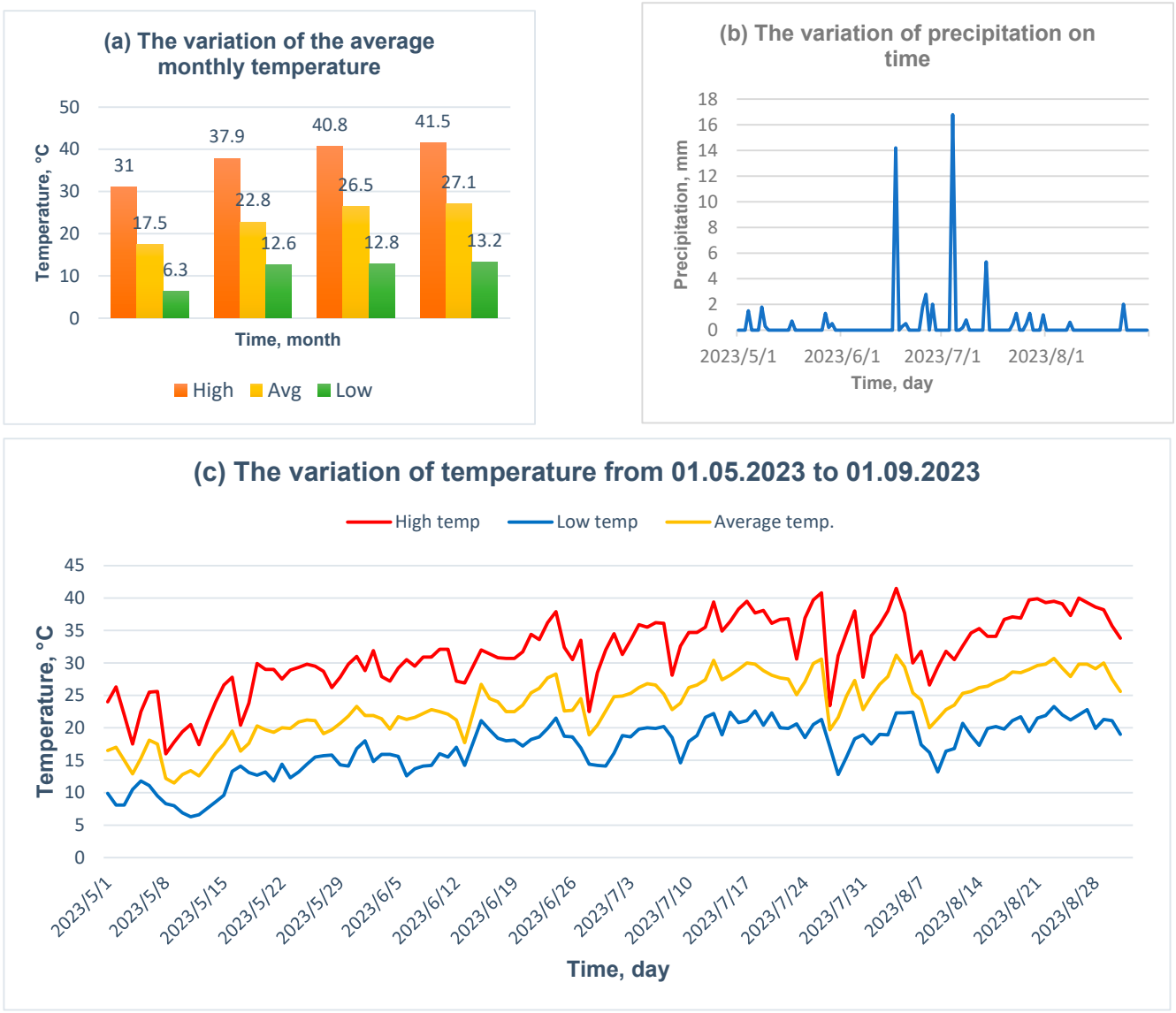

Figure 6. The meteorological data: (**a**) the variations in the highest, average, and lowest temperatures recorded in May, June, July, and August 2023, (**b**) the variations in the precipitation recorded from 1 May 2023 to 1 September 2023, and (**c**) the variations in highest, average, and lowest daily temperatures.

The research focused on plant species native to Romanian grasslands and pastures, which are naturally adapted to the local climate conditions. However, they experience significant heat stress when temperatures rise above 30 °C, with the effects becoming more severe as temperatures approach 35 °C. Within this group, *Festuca arundinacea* is noted for its relative resilience, being able to endure the higher end of this temperature range (up to 35 °C) better than the other species studied.

Higher temperatures can lead to increased evaporation rates, reducing the soil moisture content, which in turn affects the soil-water retention curve. This relationship is crucial for vegetated soils where plant roots interact with soil moisture dynamics.

As noted in [27], temperature influences both the water retention capacity and the hydraulic conductivity of rooted soils. Their model incorporated the combined effects of temperature and root presence on soil hydraulic properties, demonstrating that higher temperatures can enhance soil drying, leading to decreased water retention, particularly in the near-surface layers. This change can reduce soil cohesion, increasing the risk of desiccation cracks and potentially destabilizing slopes.

Furthermore, the authors of [28] explored non-isothermal conditions, showing that temperature gradients can influence gas and moisture transport in unsaturated soils. Their findings are crucial in the context of climate change, where fluctuating temperatures could exacerbate soil moisture variability, especially in regions with vegetated slopes. Understanding these interactions is vital for predicting slope stability under changing climatic conditions.

At the same time, it has been observed that changing the precipitation regime can disrupt the distribution of precipitation globally, intensifying erosion phenomena in some areas and substantially changing the water supply of soil in other areas, all of which leads to land degradation [29].

Short-term heavy precipitation has become an important early warning indicator of rain disasters because extreme rainfalls represent a primary factor in soil erosion and sediment yield. The latest flooding disaster in Europe in September–October 2024 was caused by short-term heavy precipitation in the catchment area of rivers associated with a major river. The floods in southern Germany, Poland, and Croatia were associated with the Danube.

3. Results and Discussions

3.1. Optimum Organic Soil Thickness

To understand how plants develop in different thicknesses of organic and sandy soil, visual observations were made on the cylinders filled with soil and sown with herbaceous seeds presented in this paper. The tests started on 30 September 2022 by seeding Mix 1 and Mix 2 (in single and double numbers of seeds) cylindrical containers. The seeds germinated after 4 days, on 3 October 2022. Conducting this experimental program was essential for designing and correctly selecting the optimal mixtures to be sown in the erosion control chamber (transparent boxes with a length of 1.05 m, thickness of 0.20 m, and height of 0.63 m), as well as determining the optimal thickness of the OS layer for both the development of the plant root system and the improvement of shear strength parameters for the soil-root system and at the soil–sand interface.

From sowing until 2 November 2022, the plants were watered with 50 mL of water every 3–4 days. On 2 November 2022, it was observed that the plants were showing signs of slight water stress, and the watering rate was increased to 100 mL for the devices with 20, 15, and 10 cm of topsoil, while it remained 50 mL for those with 5 and 0 cm of topsoil (Figure 7). The watering interval remained constant. Starting on 24 November 2022, the watering rate was increased to 150 mL for the devices with 20, 15, and 10 cm of topsoil and 100 mL for those with 5 and 0 cm of topsoil, with the remaining watering interval unchanged.

From visual observations and measurements of growth parameters from 30 September 2022 to 27 February 2023 (170 days), it was concluded that in the cylinders where a double number of seeds was sown, the results were not relevant to the research project because the density of the sprouted plants was too high, causing the plants to crowd each other and preventing proper root development. It was also observed that the plants that developed in the container with 5 cm of topsoil developed roots as strong as the plants developed in thicker layers of topsoil; this led to the conclusion that a layer of 5 cm of topsoil was optimal for the development of plants and their roots.

Based on visual observations at the end of the growth of plants, it was noticed that regardless of the seed quantity sown, the plants and roots developed similarly, with no significant differences in growth or density.

The roots of herbaceous plants act as natural reinforcements, enhancing the mechanical properties of soil. This is especially important in shallow soil layers, where herbaceous roots most effectively stabilize the surface. The roots also absorb significant amounts of water from the soil, reducing the soil moisture content. These plants are generally fast growing and have the ability to adapt to different environmental conditions, making them a flexible choice for slope stabilization projects [30].



Figure 7. The growing plants' stages at different periods: (**a**) 30 September 2022 (day 0), (**b**) 25 October 2022 (25 days), (**c**) 19 November 2022 (50 days), (**d**) 14 December 2022 (75 days), and (**e**) 27 February 2023 (150 days).

Similar research conducted by Li et al. in 2024 indicated that the roots of herbaceous plants significantly impact the biological reinforcement of slopes, particularly due to their ability to strengthen the soil structure. Additionally, the researchers found that the density and depth of the root system are essential factors in improving soil stability. Plants with deeper and denser roots provide greater protection against shallow landslides than those with smaller roots [31].

3.2. Roots Characteristics

Root system development when the OS layer varied between 0 and 20 cm was analyzed. Figure 8 presents a comparison between manually measured root lengths and WinRHIZO measurements.

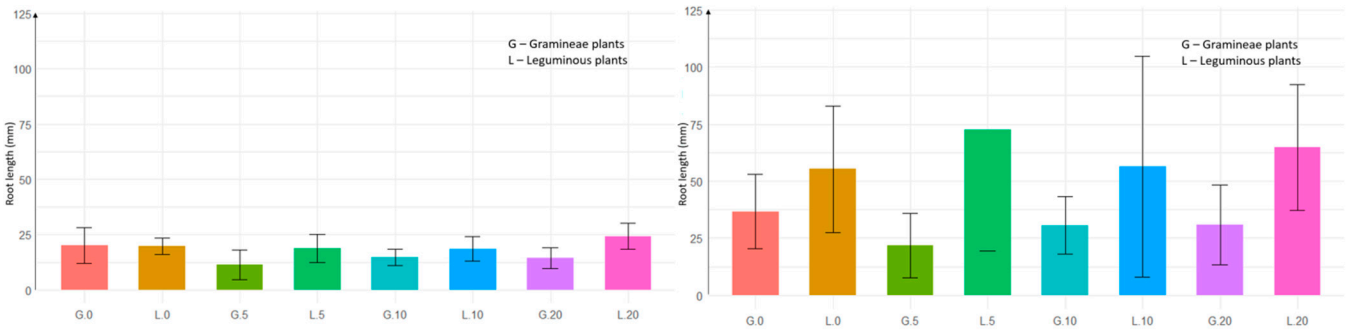

(**a**) (**b**)

Figure 8. The comparison of the influence of the OS layer thickness on root length (mm) measured (**a**) manually, and (**b**) with WinRHIZO.

When we measured the absolute length of the roots, all of the variants presented similar values. The WinRHIZO-measured lengths showed differences between Gramineae (G) and Leguminous (L) plants, and its method considered all of the segments, not only the direct line between the starting and ending points of the root systems. Gramineae plants presented lower values than Leguminous plants. The Gramineae plants grown in 5 and 10 cm OS layers (G5 and G10) had lower length values than those grown in 0 and 20 cm (G0 and G20), and Leguminous plants grown in 0 and 10 cm OS layers (L0 and L10) presented lower root developments (Figure 9).

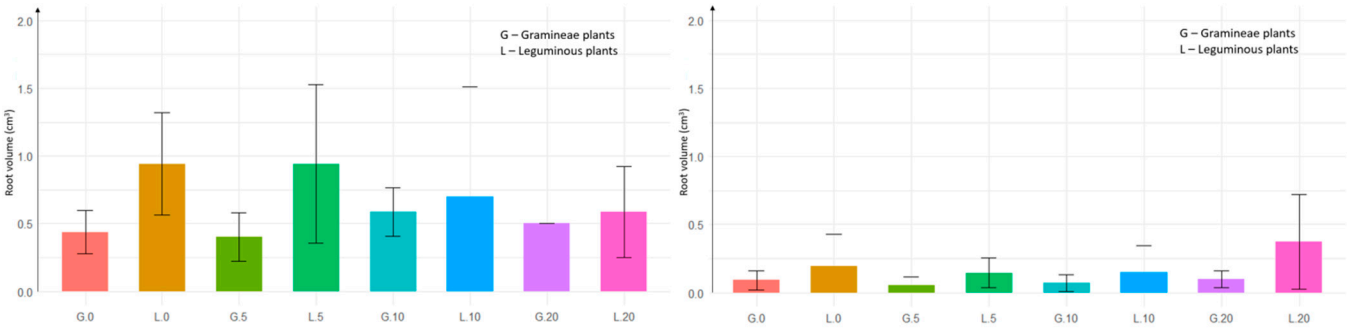

(**a**) (**b**)

Figure 9. The comparison of the influence of the OS layer thickness on root volume (cm^3) measured (**a**) manually, and (**b**) with WinRHIZO.

The WinRHIZO measurements were slightly lower than the manual ones for analyzing the root volume due to the method's specificity and digital precision. For Gramineae plants, those grown in 0 and 5 cm OS layers (G0 and G5) showed slightly lower values than those grown in 10 and 20 cm OS layers (G10 and G20). For Leguminous plants, those grown in 10 and 20 cm OS layers (G10 and G20) exhibited lower root development. The results differed from those of Pang et al. (2009) [24] but were similar to those of Wang and Zhang (2009) [32], which had differences between different volume method measurements.

The density of roots is significant; it has been observed that soil loosening occurs after a specific root density value is reached [33,34]. Kaushal et al. (2020) studied the variation in root density at depths of 0–0.90 m for different bamboo species. The study found that bamboo species with higher root densities contributed significantly to soil

reinforcement, water retention, and the overall enhancement of soil properties, making them highly effective for soil conservation in the Western Himalayan foothills [35].

Research conducted on four types of herbaceous species by Gobinath et al. (2020) showed that roots with high tensile strength and good cellulose content act as an excellent reinforcing agent for hill slope stability [36].

3.3. Shear Strength Characteristics

Direct shear tests were performed to assess the shear strength of various soil types. Samples were taken from different layers, as shown in Figure 10. These included bare sand (without vegetation)—BS, sand reinforced by plant roots—SR, bare OS—BO, OS with roots—OSR, and samples positioned at the boundary between the OS and sand layers where roots were present—INT. The results enabled a comparison of how roots and soil compositions influence shear resistance (Figure 11 and Table 1).

Table 1. The shear strength parameters of bare soil and soil with roots [37].

Shear Strength	Sandy Samples				
	BS	**SR 0–5**	**SR 10–15**	**SR 20–25**	**SR 21–25**
c (kPa)	1.24	23.43	26.3	10.65	23.52
c_r (kPa)	-	22.19	25.06	9.41	22.28
Φ (°)	32.94	32.35	30.02	30.26	32.12
Shear Strength	**OS Samples**				**Interface Samples**
	BO	**OSR 0–5**	**OSR 0–5**	**OSR 10–15**	**INT 10–15**	**INT 19–21**
c (kPa)	36.11	29.72	29.91	25.93	23.98	26.2
c_r (kPa)	-	−6.39	−6.2	−10.18		
Φ (°)	19.57	35.21	33.25	30.73	31.89	33.25

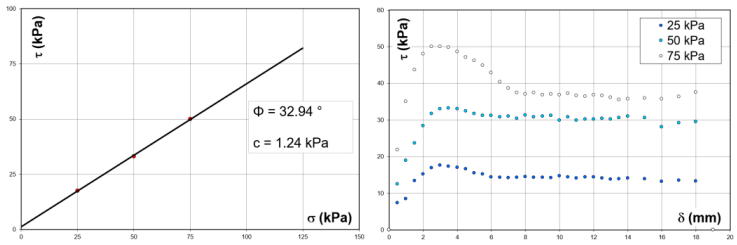

(**a**) bare sand (BS)

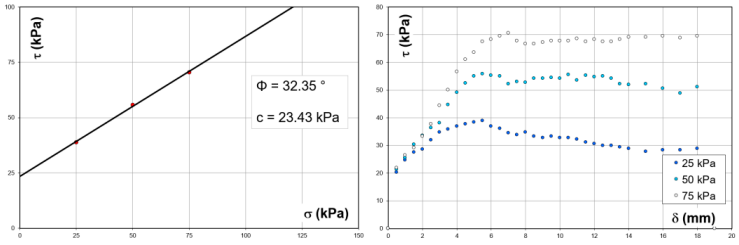

(**b**) sand with roots, sample collected from 0–5 cm depth (SR 0–5 cm)

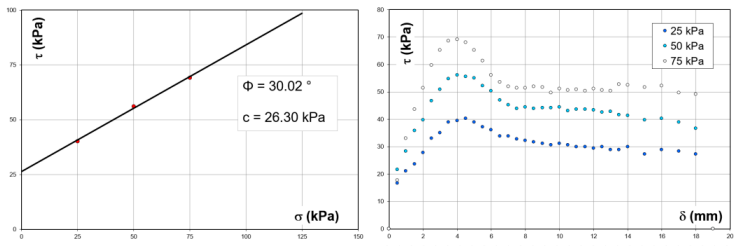

(**c**) sand with roots, sample collected from 10–15 cm (SR 10–15 cm)

Figure 10. *Cont.*

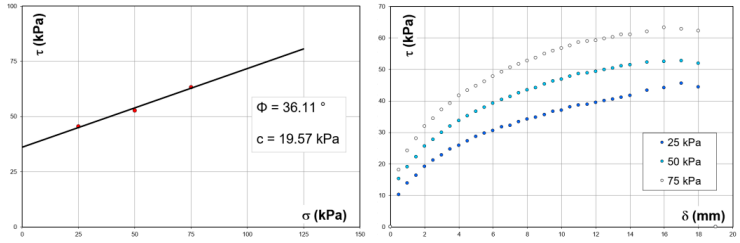

(**d**) bare organic soil (BO)

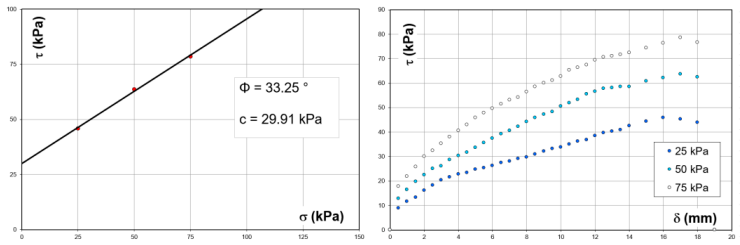

(**e**) OS with roots, a sample collected from 0–5 cm (OSR 0–5 cm)

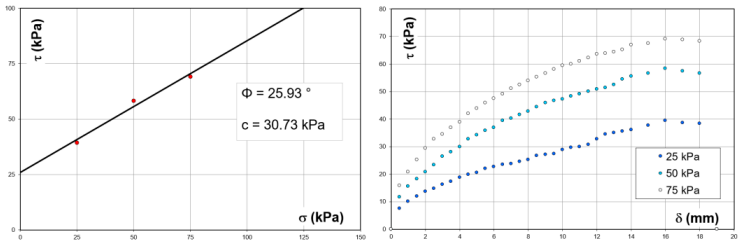

(**f**) OS with roots, sample collected from 10–15 cm (OSR 10–15 cm)

Figure 10. Variations in shear stress vs. normal stress (**left**) and shear strength vs. horizontal displacement (**right**) on soil/soil-root samples [37].

The sand was slightly compacted, which allowed it to develop both peak and residual strength values (Figure 10a–c). By contrast, the topsoil was in a loose state because it could not be compacted, resulting in no peak strength value (Figure 10d–f).

The experimental results indicated that the presence of roots introduced cohesion added by roots (c_r) when the mechanical behavior at failure was described using Mohr–Coulomb's law. At the same time, the shear strength angle (ϕ) remained in the same range. The summary of the results from the direct shear tests is presented in Table 1.

The results of the direct shear tests indicated that cohesion in sandy soils was significantly improved by the presence of root systems, increasing from 1.24 kPa for bare sand (BS) to a peak value of 26.3 kPa for the SR 10–15 sample. The internal friction angle exhibited minor fluctuations, decreasing from 32.94° in BS to 30.02° and 30.26° in SR samples extracted from depths of 10–15 cm and 20–25 cm, respectively.

For organic soil samples, the maximum cohesion value of 36.11 kPa was observed in the bare sample (BO), while a decrease to 29.91 kPa and 25.93 kPa was recorded for the OSR samples. This decrease was attributed to the loosening effect caused by roots, which reduced soil compaction. However, the internal friction angle improved significantly in the OSR samples compared to the BO samples.

For interface samples taken between organic soil and sand in the presence of roots, the cohesion values were comparable to those of SR samples but lower than those of OSR samples. The internal friction angle did not show significant differences compared to samples with roots. Notably, interface samples tended to maintain the most favorable shear strength characteristics from both sandy and organic soil samples, combining the strengths of both materials effectively.

Cazzuffi et al. (2014) conducted direct shear tests on soil samples (63.3% silt and 28.7% clay) with roots (from the family *Gramineae*) and observed that the reinforcing effect provided by roots only added an increment of cohesion. The cohesion of the root-soil

system was significantly higher than that of the bare soil (i.e., about 72% for *Atriplex canescens*). The results indicated an increase in shear strength due to root reinforcement of approximately 25% (for *Atriplex canescens*) compared to the shear strength of soil without roots [13].

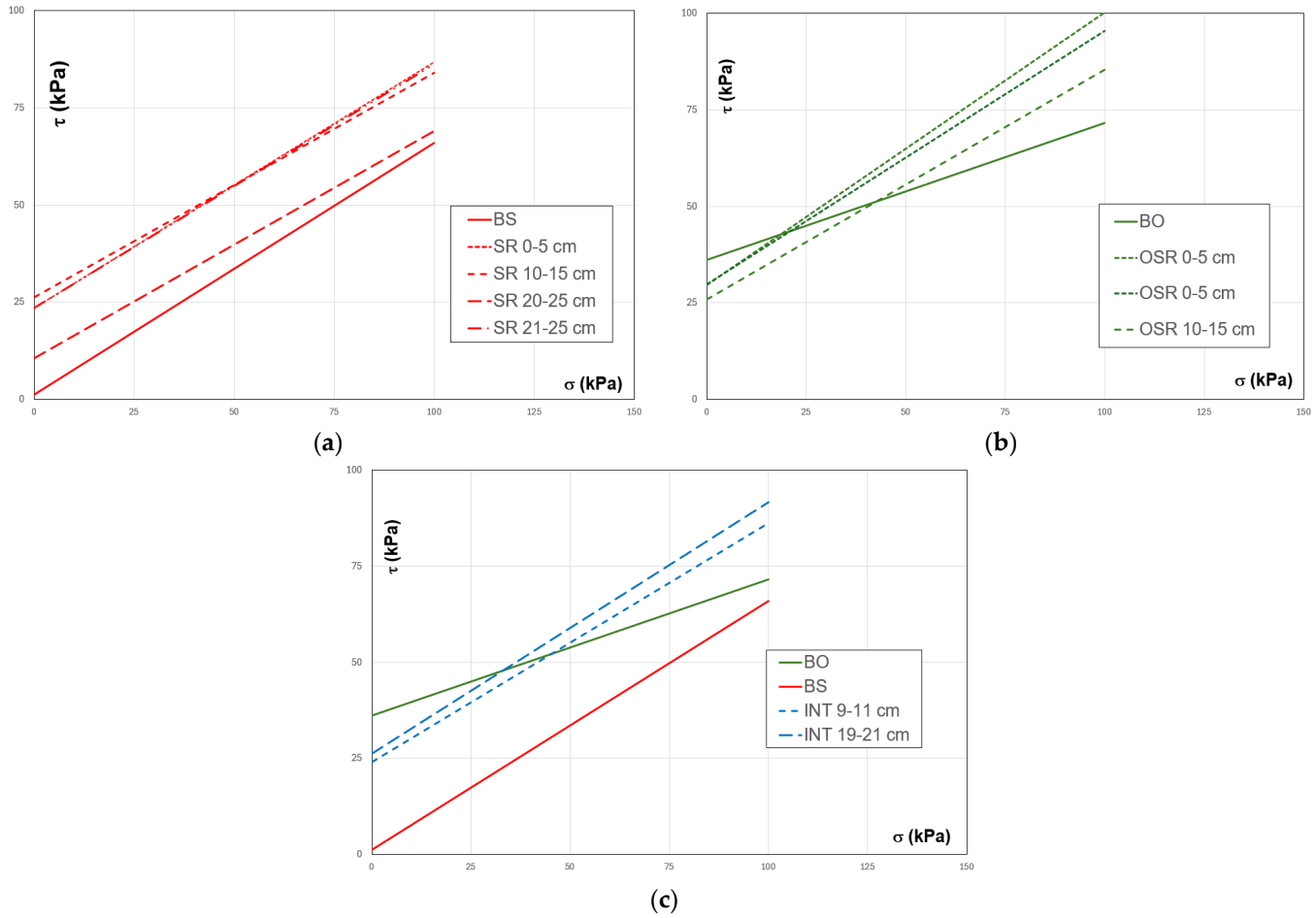

Figure 11. The variations in shear stress vs. normal stress on all analyzed samples: (**a**) sandy samples, (**b**) OS samples, and (**c**) samples collected from the interface between OS and sand [37].

Zhang et al. (2023) noticed that rainwater infiltration is crucial for rainfall-induced slope failure because the infiltrated water can significantly weaken the shear strength of unsaturated soil [18]. This conclusion was in relation to the UUsat tests conducted in our study.

Based on the shear strength parameters, slope stability is evaluated; the more significant the internal friction angle and the cohesion of rooted soils, the higher the slope's stability factor. Research conducted by Li et al. (2022) showed that the shear strength parameters of rooted soils increase with the growth of root diameter. They also examined four models of root distribution in soil, specifically with distribution angles of 0°, 30°, 60°, and 90°. The vertical root distribution model in the soil at a 90° distribution angle could increase cohesion by up to 150% [31]. In our paper, the shear strength parameters were determined on natural roots, developed naturally with a distribution angle of 90°; in conclusion, all of the shear strength parameters determined were at the maximum increase value.

Tang et al. (2023) performed triaxial shear tests to observe how palm fibers affected the mechanical properties of a sandy sample. The tests were carried out under consolidated drained conditions (C.D.), and the research included 16 series of remolded palm fiber-reinforced sand samples and one series of bare sand for comparison. The study varied

fiber lengths between 8 mm and 20 mm and fiber contents between 0.3% and 0.9% by mass. The results indicated that while palm fibers contributed significantly to the critical shear strength (increasing by over 100%), they had a more modest effect on peak shear strength (increasing by about 10–20%). The analysis revealed that fiber-reinforced sand experienced different volume changes and void ratios than bare sand. The fiber content was positively correlated with increased strength capacity, but it was recommended to determine the shear strength parameters on naturally grown roots not remolded samples [38].

3.4. Erosion Tests Under Rainfall Conditions

The tests conducted using the experimental model, which simulated the effect of torrential rainfall of 400 L/s·ha (144 mm/h) on a slope of 2:3 (V:H) at scale, focused on assessing the changes in the slope profile over time.

In Romania, the STAS 9470-73 standard provides intensity-duration-frequency (IDF) curves for rainfall events with the highest intensity of 500 L/s·ha and return periods ranging from 1 to 50 years. A rainfall intensity of 400 L per second per hectare corresponds to an event with a 20-year return period and a duration of 20 min [39]. Under the current conditions of climate change, the tests were performed for periods of time longer than 20 min.

For the test performed on an unprotected sandy slope, it was observed that after a maximum of 20 min of rainfall, the slope experienced complete degradation, with the material being eroded and the slope reaching a gradient of approximately 1:5.5 (V) (Figure 12). The rainfall was applied for 30 min.

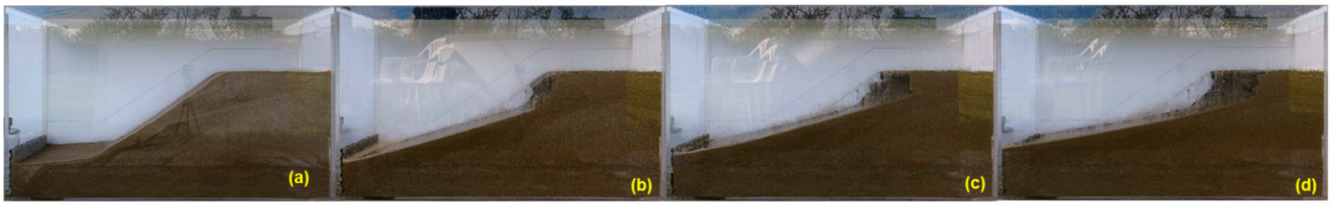

Figure 12. Variations in the profile of the unprotected sandy slope during a rainfall simulation for different periods [26]: (**a**) t = 0 min, (**b**) t = 10 min, (**c**) t = 20 min, and (**d**) t = 30 min.

When geosynthetic materials were used for erosion control, the onset of erosion was delayed, varying in effectiveness depending on the specific materials applied (Figures 13–15). It was observed that erosion caused by raindrops was practically eliminated, as the shape of these geosynthetic materials is specifically designed for this purpose. The displaced material was carried underneath the geosynthetic material because the soil mass was fully saturated during the rainfall simulation. The rainfall was applied for 30 min in the case of the slope protected by GEC 2 and 40 min in the case of the slopes protected by GEC 1 and GEC 3. It was decided not to display the captures after 40 min of rainfall because the geometry of the slope remained approximately the same, the amount of eroded material was roughly the same, and it was decided that all of the representations in Figures 13–15 should be on the same scale.

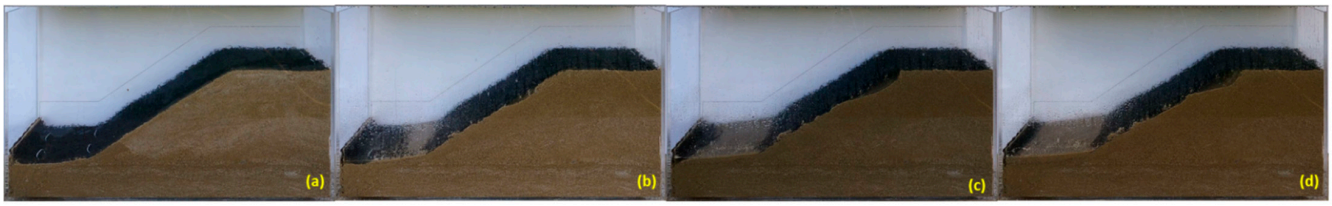

Figure 13. The variations in the profile of a sandy excavation unprotected and protected with GEC1 during rainfall simulation for different periods [26]: (**a**) t = 0 min, (**b**) t = 10 min, (**c**) t = 20 min, and (**d**) t = 30 min.

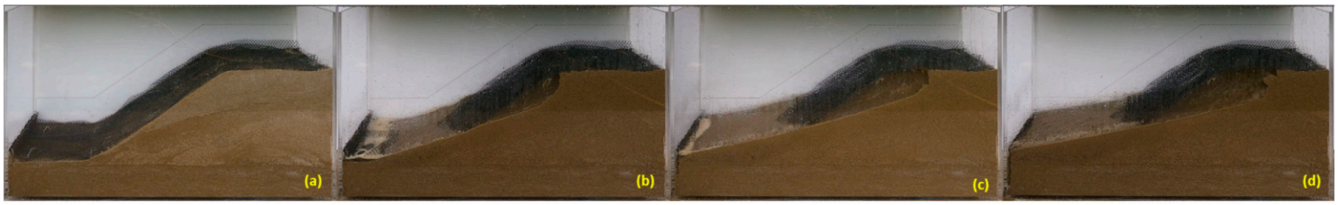

Figure 14. The variations in the profile of a sandy excavation unprotected and protected with GEC2 during rainfall simulation for different periods [26]: (**a**) t = 0 min, (**b**) t = 10 min, (**c**) t = 20 min, and (**d**) t = 30 min.

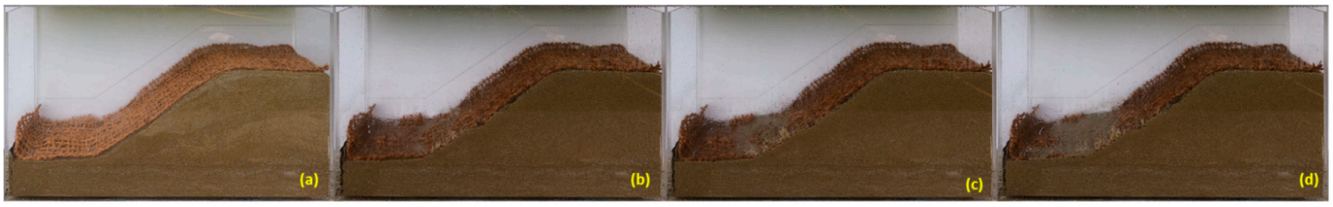

Figure 15. The variations in the profile of a sandy excavation unprotected and protected with GEC3 during rainfall simulation for different periods [26]: (**a**) t = 0 min, (**b**) t = 10 min, (**c**) t = 20 min, and (**d**) t = 30 min.

From the scaled model tests shown in Figures 12–15, it can be observed that surface runoff was significantly reduced compared to the bare sand model (unprotected slope) when GEC1 and GEC3 were used. The use of GEC2 showed only a slight delay in runoff compared to the unprotected slope but was far less effective than the use of GEC1 and GEC3. This was due to the larger mesh openings of GEC2 compared to those of GEC1 and GEC3. Additionally, it was noted that GEC3, made of biodegradable natural fibers, expanded in volume upon hydration, effectively reducing soil loss by limiting raindrop impact. These experiments showed a noticeable decline in erosion rates when geosynthetic materials were used to protect the sandy slope.

A similar study conducted by He et al. (2023) revealed that sandy soil is the most problematic soil in terms of soil erosion. The research concluded that slope instability in the study area was primarily due to the soil's geotechnical properties, particularly its high permeability and low shear strength. Rainfall is critical in accelerating instability, especially under prolonged or intense conditions. The treatment measures implemented (geosynthetics and vegetation) successfully improved slope stability [40].

For the same slope, protected by a thin layer of 0.5 cm of OS and immature vegetation, no significant improvement was observed under similar rainfall conditions compared to the other tests (the unprotected slope or the slope protected by only a thin layer of OS layer). The seeds were planted on 15 April 2023, and the torrential rainfall simulation was conducted on 14 May 2023, just one month after sowing. The vegetation exhibited minimal, anemic growth, as the plants had only a very thin layer of topsoil of 0.5 cm (Figure 16). This stunted growth was correlated with the development of very thin, superficial roots, as validated in the cylindrical containers discussed in Section 3.1.

Simulated torrential rainfall over an area where excavation had been made in sandy soil, topped with a layer of 5 cm of OS that had been seeded but where vegetation had not yet developed, had severe effects. In the scaled model, landslides occurred, completely altering the initial profile after just 10 min of intense rainfall (Figure 17).

This rapid and massive shallow landslide occurred because the topsoil without plant roots absorbed all of the rainwater quickly, increasing its weight. Since the soil beneath the topsoil layer was not saturated, a failure plane formed below the saturated topsoil layer, causing a general instability in 10 min. The scaled model test remained undisturbed during the winter, from January 2023 until April 2023. Because during the winter of 2023–2024 there were a few days with below-freezing temperatures, the seeds germinated, sprouted,

and grew. It was observed that during the landslide caused by the torrential rainfall simulation, the seedlings also slid to the base of the slope.

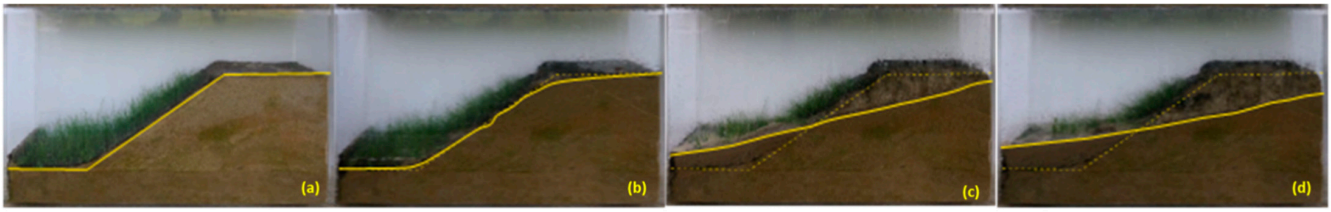

Figure 16. The variations in the profile of a sandy excavation protected by 0.5 cm of OS with immature vegetation during rainfall simulation for different periods [26]: (**a**) t = 0 min, (**b**) t = 10 min, (**c**) t = 20 min, and (**d**) t = 30 min.



Figure 17. The variations in the profile of a sandy excavation protected by 5 cm of OS (with seeds) during rainfall simulation for different periods: (**a**) t = 0 min, (**b**) t = 10 min, and (**c**) after approx. four months, during the winter.

To observe the effect of rainfall simulation on slopes protected with 5 cm OS, vegetation, and geosynthetic materials, four erosion chambers were placed in an experimental plot located in Chiajna, Ilfov County, Romania. They were exposed to natural climatic humidity and temperature conditions from 1 May 2023 to 1 September 2023. Their evolution in two important stages can be observed in Figures 18 and 19.

The effect of mature vegetation on slope stability can be observed in Figure 20. For this test, a seed mixture was planted on 1 May 2023, consisting of *Festuca arundinacea* (25%), *Dactylis glomerata* (25%), *Phleum pratense* (20%), *Trifolium pratense* (10%), and *Trifolium repens* (20%), over a 5 cm thick layer of OS. The rainfall simulation was conducted on 15 June 2023, one and a half months after the seeds were sown. The rainfall simulation was applied at the most unfavorable time possible after trimming the plants. It was observed that mature vegetation was very effective in controlling slope erosion. After the rainfall simulation, the slope of the embankment remained the same, and no signs of erosion appeared, even after 50 min.

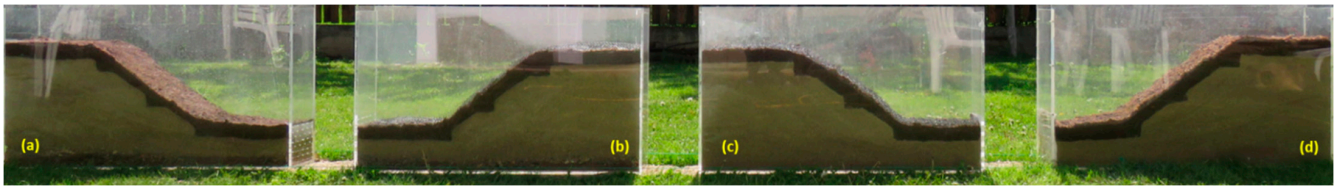

Figure 18. The sandy slope protected by 5 cm OS layer after seeding (1 May 2023): (**a**) slope protected by 5 cm OS, (**b**) slope protected by 5 cm OS and GEC 1, (**c**) slope protected by 5 cm OS and GEC 2, and (**d**) slope protected by 5 cm OS and GEC 3.

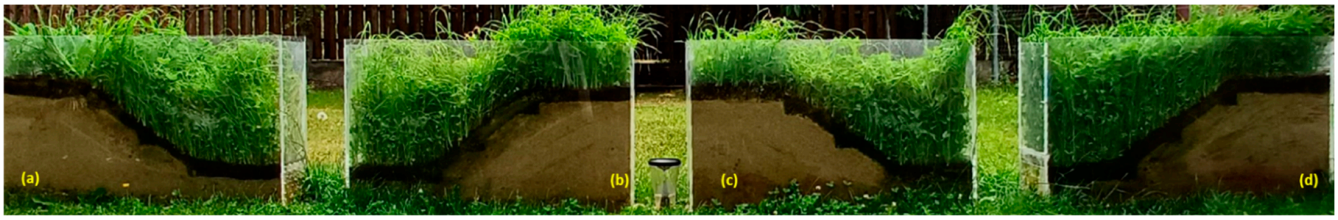

Figure 19. The sandy slope protected by a 5 cm OS layer and mature vegetation after 45 days of seeding (15 June 2023): (**a**) slope protected by 5 cm OS, (**b**) slope protected by 5 cm OS and GEC 1, (**c**) slope protected by 5 cm OS and GEC 2, and (**d**) slope protected by 5 cm OS and GEC 3.

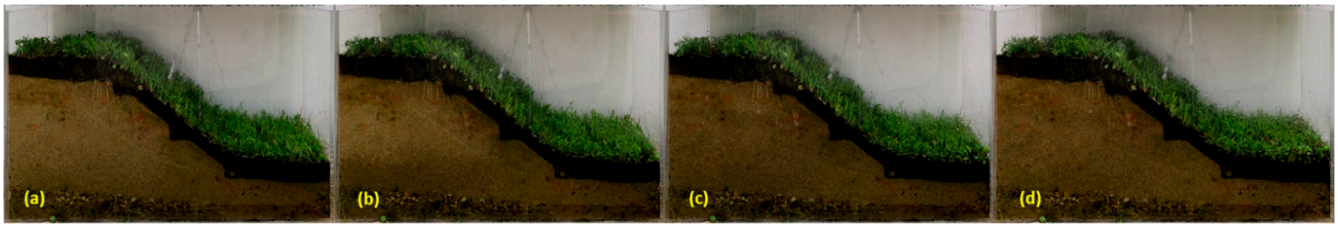

Figure 20. The variations in the profile of a sandy excavation protected by 5 cm of OS with trimmed mature vegetation during rainfall simulation for different periods: (**a**) t = 0 min, (**b**) t = 10 min, (**c**) t = 30 min and (**d**) t = 50 min.

The soil loss was nearly zero when rainfall simulations were applied to the sandy excavation protected by a 5 cm OS layer and mature vegetation. Similar tests were not conducted for the sandy excavation protected by a 5 cm OS layer, mature vegetation, and geosynthetics for erosion control, as it was assumed that soil loss would also be nearly zero under rainfall simulation conditions. The same results were obtained by Artidteang et al. in field tests [41].

Similar experiments conducted by Zhao et al. examined the combined effects of rainfall intensity and slope gradient on soil erosion, runoff, and infiltration. For example, experiments using a rainfall simulator showed that higher rainfall intensities and steeper slopes significantly increase soil erosion and surface runoff, while reducing infiltration rates. This study emphasized the critical role of land management, particularly in sloped agricultural areas, to mitigate soil degradation and water loss. Such research is crucial for developing sustainable agricultural practices that reduce soil erosion and nutrient leaching, thereby protecting soil health and water resources [42].

This test was conducted under the most favorable conditions, when temperatures supported plant growth and development and water needs were met by precipitation or irrigation. Unfortunately, the effects of climate change were also felt by these plants, leading them to dry out by the end of the summer. To observe how plants were influenced by the increased summer temperatures and the drought caused by the lack of precipitation, the grass-covered slopes were left in natural temperature and humidity conditions until 1 September 2023. During this period, there were 78 days with temperatures exceeding 30 °C and 60 mm of precipitation. These climatic conditions caused the plants to dry out, allowing for simulations of torrential rains under the most unfavorable situation: mature, dry vegetation (Figure 21).

In Figures 21–25, continuous red lines are drawn to indicate the surface of the profile (the upper layer of the topsoil). There were no changes in the position of this line under heavy rainfall. Dotted yellow lines are used to show the profile of the upper part of the sandy soil, which initially marks the interface between the sandy soil and topsoil. However, under heavy rainfall, this sandy soil profile significantly changed at the interface with the plexiglass due to the formation of cracks measuring 0.3 to 0.5 mm.

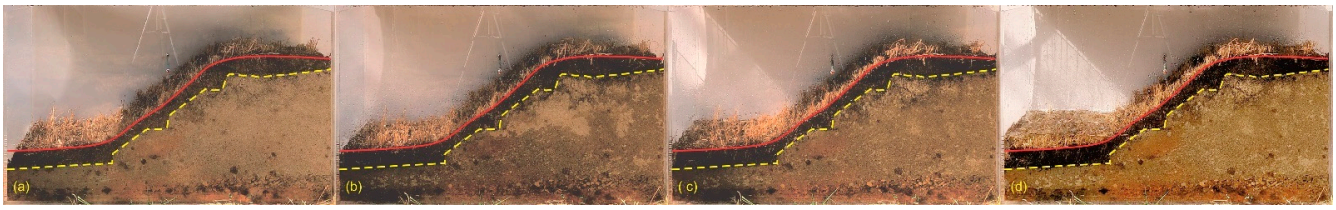

Figure 21. The variations in the profile of a sandy excavation protected by 5 cm of OS with dried mature vegetation during rainfall simulation for different periods: (**a**) t = 0 min, (**b**) t = 10 min, (**c**) t = 30 min and (**d**) t = 50 min.



Figure 22. The variations in the profile of a sandy excavation protected by 5 cm of OS with dried mature vegetation during rainfall simulation for different periods: (**a**) t = 0 min, (**b**) t = 80 min, (**c**) t = 100 min and (**d**) t = 120 min.

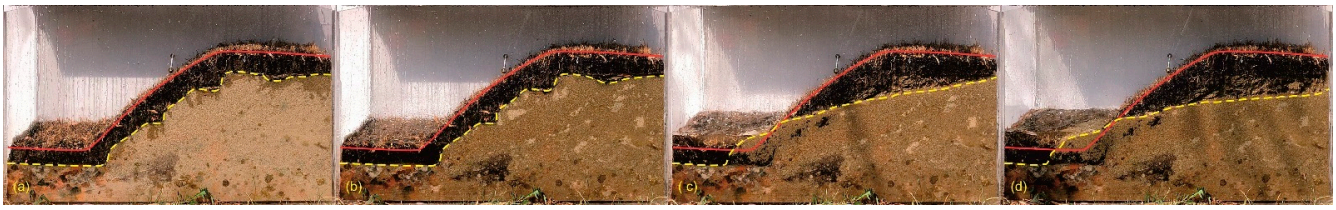

Figure 23. The variations in the profile of a sandy excavation protected by 5 cm of OS with dried mature vegetation and GEC 1 during rainfall simulation for different periods: (**a**) t = 0 min, (**b**) t = 10 min, (**c**) t = 30 min and (**d**) t = 50 min.

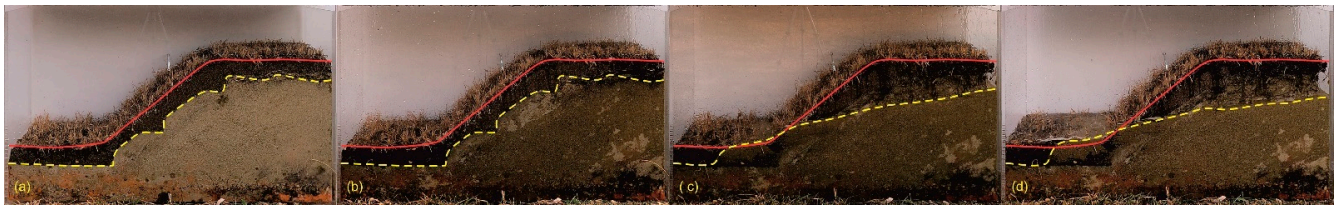

Figure 24. The variations in the profile of a sandy excavation protected by 5 cm of OS with dried mature vegetation and GEC 2 during rainfall simulation for different periods: (**a**) t = 0 min, (**b**) t = 10 min, (**c**) t = 30 min and (**d**) t = 50 min.



Figure 25. The variations in the profile of a sandy excavation protected by 5 cm of OS with dried mature vegetation and GEC 3 during rainfall simulation for different periods: (**a**) t = 0 min, (**b**) t = 10 min, (**c**) t = 30 min and (**d**) t = 50 min.

During the rainfall simulations on the slope protected by 5 cm of OS and mature dry vegetation, it was observed that the sand was displaced on the side opposite to the filmed

area after approximately 75 min, and the camera was moved. Figure 22 shows the amount of displaced material.

The samples were irrigated and developed in the first two weeks after sowing, reaching maturity approximately one and a half months after sowing. After this period, they were left at natural environmental humidity and temperature (as shown in Figures 21–25) during a summer period characterized by high temperatures and no recorded precipitation. Under these conditions, the topsoil contracted, and upon contact with the plexiglass walls of the erosion chamber, cracks of 0.3–0.5 mm formed. In the simulated torrential rain tests, no erosion was recorded in the entire soil mass, even with dry vegetation (Figures 21–25). Still, sand was displaced in the interface areas with the plexiglass wall.

The study conducted by Deng et al. underscored the importance of understanding the complex interactions between vegetation dynamics and hydrological processes, particularly in the context of climate change and environmental management strategies. They highlighted that soil (mainly from grasslands) dried in 65.87% of global vegetation greening areas. By using remote sensing data and climate models, the research contributes to a nuanced understanding of how greening impacts soil–water relations, offering insights that are crucial for developing adaptive land management practices in drylands [43].

Similar research conducted by Tolz and Wagenbrenner focused on post-fire erosion control using geosynthetics in combination with vegetation cover. Using simulated rainfall events on scaled plots, the study assessed the effectiveness of different erosion control products, including biodegradable mats and synthetic covers, in reducing soil loss and promoting vegetation establishment. The results showed that integrating geosynthetics with vegetation can significantly lower erosion rates in vulnerable slopes, particularly in post-disturbance environments [44].

Integrating temperature effects into scaled model tests of soil hydraulic behavior is essential for accurately predicting slope stability, especially for vegetated slopes. In our future studies, we should continue to explore these dynamics to improve slope management practices in a warming climate.

Research on soil massive erosion will be further developed by replacing the sand with loess (also a very erodible soil)—a soil sensitive to moisture (a material that covers approximately 18% of Romania's territory, according to NP 125:2010 [45])—and a clayey material, predominantly used in earthworks. Another research directive will focus on modeling the scaled tests through stability calculations using limit equilibrium and finite element analysis. It was noticed that life cycle cost analysis has recently gained significant importance, and the researchers aim to explore this parameter in their future studies.

4. Conclusions

Vegetation as a bio-reinforcement method is often more cost effective and environmentally friendly than traditional engineering solutions, such as concrete. However, this bio-stabilization approach is unsuitable for applications requiring deep stabilization.

Bio-stabilization techniques contribute to the ecological restoration of slopes by supporting biodiversity and improving the aesthetic value of landscapes. The selection of appropriate species and planting techniques depends on the area's specific soil and climate conditions to ensure optimal root development and stabilization efficiency. Vegetation can be combined with other mechanical stabilization methods for hybrid approaches to slope management.

The roots of plants play a crucial role in stabilizing slopes by improving soil cohesion, reducing water content, and providing long-term reinforcement, making them a valuable natural solution for slope erosion control.

Based on the direct shear tests conducted in this study, an increase in the cohesion for sandy samples was registered from 1.24 kPa for BS to a peak value of 26.3 kPa for SR, representing a significant improvement of 2020% due to the presence of root systems. In terms of the internal friction for sandy samples, a reduction of 8–9% was recorded due to the presence of roots. For the organic soil samples, a decrease in cohesion of 28% was

recorded due to loosening (root-induced loosening effect) from BO to OSR samples; while the friction angle registered a substantially increase of 57% to 80% for OSR compared to BO samples. For the samples collected at the interface between OSR and SR, the cohesion had comparable values to SR samples but was lower than OSR samples. In the terms of the internal friction angles, no significant differences were observed. The presence of roots significantly enhanced cohesion in sandy soil, with the peak improvement at root depths of 10–15 cm. Organic soil samples registered a reduced cohesion but a significant increase in the internal friction angle. And the samples situated at the interface achieved a balance between the strengths of the sandy and organic soils, combining moderate cohesion and consistent friction angle values.

In designing artificial slopes, an important stability analysis should be conducted for the scenario where the vegetation has dried out following a drought period. This scenario does not correspond to the scenario without vegetation, as the plant roots remain fixed in the soil and can regenerate after rainy periods.

The authors of this paper support the use of targeted vegetation management as a sustainable engineering solution for slope stabilization, particularly in regions susceptible to landslides and soil erosion. Vegetation provides long-term soil reinforcement through root systems, but this approach requires support during the initial establishment phase.

Geosynthetic materials play a crucial role during the early stages, before vegetation and root systems are fully developed, by minimizing the impact of raindrops and stabilizing seeds to promote uniform plant growth. Once this critical period passes and the soil becomes reinforced by plant roots, the importance of geosynthetics diminishes.

Therefore, biodegradable (made by natural fibers) geomats are also used for enhanced erosion control. This biodegradable material is highly effective immediately after installation, absorbing the water used to irrigate the slope and maintaining a surface moisture level in the topsoil that is conducive to plant germination (faster than other used materials). This is particularly important in non-agricultural areas where no additional irrigation is applied after installation. This property, combined with the fact that it is made from natural fibers, makes it an environmentally friendly and sustainable material.

The scaled model tests further underscored the effectiveness of geosynthetics on unvegetated slopes. GEC1 and GEC3 significantly reduced surface runoff compared to unprotected slopes, while GEC2 was less effective due to its larger mesh openings. These findings confirmed that geosynthetics like GEC1 and GEC3 are indispensable for early-stage erosion control, particularly in environments unsuitable for immediate vegetation establishment, ensuring stability until vegetation can independently support the soil.

The bio-stabilization of slopes or bio-reinforcement with living plants is a sustainable topic that requires the involvement of specialists in geotechnical engineering, agriculture, horticulture, environmental engineering, and landscaping.

Author Contributions: Conceptualization, T.O. and E.-D.O.; methodology, T.O., E.-D.O. and A.-C.B.; analysis, T.O., E.-D.O. and A.-C.B.; investigation, T.O. and E.-D.O.; resources, E.-D.O.; writing—original draft preparation, T.O.; writing—review and editing, T.O. and E.-D.O.; supervision, T.O. and E.-D.O.; funding acquisition, T.O. All authors have read and agreed to the published version of the manuscript.

Funding: This research was funded by The University of Agronomic Sciences and Veterinary Medicine from Bucharest, grant number 1068/15.06.2022. Acronym: GeoRoots.

Institutional Review Board Statement: Not applicable.

Informed Consent Statement: No humans were involved in this study.

Data Availability Statement: The data used in this study are available upon request from the corresponding author, as they are subject to privacy and ethical restrictions. Public access is not possible due to confidentiality agreements with the research participants.

Conflicts of Interest: The authors declare no conflicts of interest.

References

1. Fatema, N.; Ansary, M. Slope stability analysis of a Jamuna River embankment. *J. Civ. Eng.* **2014**, *42*, 119–136.
2. Hearn, G.J.; Shakya, N.M. Engineering challenges for sustainable road access in the Himalayas. *Q. J. Eng. Geol. Hydrogeol.* **2017**, *50*, 69–80. [CrossRef]
3. Wu, W.; Switala, B.M.; Acharya, M.S.; Tamagnini, R.; Auer, M.; Graf, F.; Kamp, L.; Xiang, W. Effect of Vegetation on Stability of Soil Slopes: Numerical Aspect. In *Recent Advances in Modeling Landslides and Debris Flows*, 1st ed.; Wu, W., Ed.; Springer Series in Geomechanics and Geoengineering, International; Springer: Cham, Switzerland, 2015.
4. Masi, E.B.; Segoni, S.; Tofani, V. Root Reinforcement in Slope Stability Models: A Review. *Geosciences* **2021**, *11*, 212. [CrossRef]
5. Mao, Z.; Saint-Andre, L.; Genet, M.; Mine, F.X.; Jourdan, C.; Rey, H.; Courbaud, B.; Stokes, A. Engineering ecological protection against landslides in diverse mountain forests: Choosing cohesion models. *Ecol. Eng.* **2012**, *45*, 55–69. [CrossRef]
6. Ghestem, M.; Sidle, R.C.; Stokes, A. The influence of plant root systems on subsurface flow: Implications for slope stability. *Bioscience* **2011**, *61*, 869–879. [CrossRef]
7. Ni, J.J.; Leung, A.K.; Ng, C.W.W.; Shao, W. Modelling hydro-mechanical reinforcements of plants to slope stability. *Comput. Geotech.* **2018**, *95*, 99–109. [CrossRef]
8. Rimoldi, P. Design of geosynthetics for erosion control on slopes. In Proceedings of the 6th EuroGeo 6 Conference, Ljubljana, Slovenia, 25 September 2016; pp. 339–360.
9. Mandal, D.; Patra, S.; Sharma, N.K.; Alam, N.M.; Jana, C.; Lal, R. Impacts of Soil Erosion on Soil Quality and Agricultural Sustainability in the North-Western Himalayan Region of India. *Sustainability* **2023**, *15*, 5430. [CrossRef]
10. Singh, M.; Hartsch, K. Basics of soil erosion. In *Watershed Hydrology, Management and Modeling*, 1st ed.; Yousuf, A., Singh, M., Eds.; CRC Press: Boca Raton, FL, USA, 2019; pp. 1–61.
11. Kanianska, R.; Kizeková, M.; Jančová, Ľ.; Čunderlík, J.; Dugátová, Z. Effect of Soil Erosion on Soil and Plant Properties with a Consequence on Related Ecosystem Services. *Sustainability* **2024**, *16*, 7037. [CrossRef]
12. Turcu, C.L.; Chiper, B.M.; Bucur, D.; Popa, N. Research on runoff and soil erosion in the Tărnii Valley hydrographic basin from Tutova rolling hils, Romania, during 2019–2021. *AgroLife Sci. J.* **2024**, *13*, 217–222.
13. Cazzuffi, D.; Cardile, G.; Gioffrè, D. Geosynthetic engineering and vegetation growth in soil reinforcement applications. *Transp. Infrastruct. Geotechnol.* **2014**, *1*, 262–300. [CrossRef]
14. Mairaing, W.; Jotisankasa, A.; Leksungnoen, N.; Hossain, M.; Ngernsaengsaruay, C.; Rangsiwanichpong, P.; Pilumwong, J.; Pramusandi, S.; Semmad, S.; Ahmmed, A.N.F. A Biomechanical Study of Potential Plants for Erosion Control and Slope Stabilization of Highland in Thailand. *Sustainability* **2024**, *16*, 6374. [CrossRef]
15. Lobmann, M.T.; Geitner, C.; Wellstein, C.; Zerbe, S. The influence of herbaceous vegetation on slope stability—A review. *Earth-Sci. Rev.* **2020**, *209*, 103328. [CrossRef]
16. Cao, T.; Zhang, H.; Chen, T.; Yang, C.; Wang, J.; Guo, Z.; Sun, X. Research on the mechanism of plant root protection for soil slope stability. *PLoS ONE* **2023**, *18*, e0293661. [CrossRef] [PubMed]
17. Zhao, J.; Zhu, Z.; Zhang, D.; Wang, H.; Li, X. Assessment of fabric characteristics with the development of sand liquefaction in cyclic triaxial tests: A DEM study. *Soil Dyn. Earthq. Eng.* **2024**, *176*, 108343. [CrossRef]
18. Zhang, X.; Wang, H.; Gao, Z.; Xiang, K.; Zhai, Q.; Satyanaga, A.; Chua, Y.S. Evaluation of the Performance of the Horizontal Drain in Drainage of the Infiltrated Water from Slope Soil under Rainfall Conditions. *Sustainability* **2023**, *15*, 14163. [CrossRef]
19. Cardile, G.; Pisano, M. Advances in soil reinforcement with geosynthetics: From laboratory tests to design practice. *Riv. Ital. Geotech.* **2020**, *54*, 52–82.
20. Markiewicz, A.; Koda, E.; Kawalec, J. Geosynthetics for Filtration and Stabilisation: A Review. *Polymers* **2022**, *14*, 5492. [CrossRef]
21. Markiewicz, A.; Koda, E.; Kiraga, M.; Wrzesiński, G.; Kozanka, K.; Naliwajko, M.; Vaverková, M.D. Polymeric Products in Erosion Control Applications: A Review. *Polymers* **2024**, *16*, 2490. [CrossRef]
22. Kim, Y.-J.; Kotwal, A.R.; Cho, B.-Y.; Wilde, J.; You, B.H. Geosynthetic Reinforced Steep Slopes: Current Technology in the United States. *Appl. Sci.* **2019**, *9*, 2008. [CrossRef]
23. *SR EN-ISO 14688-2:2018*; Geotechnical Investigations and Tests. Identification and Classification of Soil. Part 2: Principles for a Classification. ISO: Geneva, Switzerland, 2018.
24. Pang, W.; Crow, W.T.; Luc, J.E.; McSorley, R.; Giblin-Davis, R.M.; Kenworthy, K.E.; Kruse, J.K. Comparison of Water Displacement and WinRHIZO Software for Plant Root Parameter Assessment. *Plant Dis.* **2011**, *95*, 1308–1310. [CrossRef]
25. *SR EN ISO 17892-10:2019*; Geotechnical Investigations and Tests. Laboratory Tests of Soils. Part 10: Direct Shear Tests. ISO: Geneva, Switzerland, 2019.
26. Olinic, T.; Olinic, E.D. The role of geosynthetic materials and vegetation on slope erosional control: Results of scale model tests. *E3S Web Conf.* **2024**, *569*, 09004. [CrossRef]
27. Wang, H.; Chen, R.; Leung, A.K.; Gui, L.J.; Wu, F. Modelling nonisothermal gas conductivity function of unsaturated rooted soils. *Int. J. Heat Mass Transf.* **2024**, *229*, 125744. [CrossRef]
28. Wang, H.; Chen, R.; Leung, A.K.; Huang, J. Temperature effects on the hydraulic properties of unsaturated rooted soils. *Can. Geotech. J.* **2023**, *60*, 936–945. [CrossRef]
29. Corches, M.T. Land degradation and climate change. *Sci. Pap. Ser. E Land Reclam. Earth Obs. Surv. Environ. Eng.* **2023**, *12*, 69–73.
30. Gong, C.; Ni, D.; Liu, Y.; Li, Y.; Huang, Q.; Tian, Y.; Zhang, H. Herbaceous Vegetation in Slope Stabilization: A Comparative Review of Mechanisms, Advantages, and Practical Applications. *Sustainability* **2024**, *16*, 7620. [CrossRef]

31. Li, P.; Xiao, X.; Wu, L.; Li, X.; Zhang, H.; Zhou, J. Study on the Shear Strength of Root-Soil Composite and Root Reinforcement Mechanism. *Forests* **2022**, *13*, 898. [CrossRef]
32. Wang, M.B.; Zhang, Q. Issues in using the WinRHIZO system to determine physical characteristics of plant fine roots. *Acta Ecol. Sin.* **2009**, *29*, 136–138. [CrossRef]
33. Bengough, A.G.; Bransby, M.F.; Hans, J.; McKenna, S.J.; Roberts, T.J.; Valentine, T.A. Root responses to soil physical conditions; growth dynamics from field to cell. *J. Exp. Bot.* **2006**, *57*, 437–447. [CrossRef]
34. Olinic, T.; Stanciu, A.M.; Butcaru, A.C.; Luchian, V. Bio-reinforcement of slopes. *Sci. Pap. Ser. E Land Reclam. Earth Obs. Surv. Environ. Eng.* **2023**, *12*, 25–30.
35. Kaushal, R.; Singh, I.; Thapliyal, S.D.; Gupta, A.K.; Mandal, D.; Tomar, J.M.S.; Kumar, A.; Alam, N.M.; Kadam, D.; Singh, D.V.; et al. Rooting behaviour and soil properties in different bamboo species of Western Himalayan Foothills, India. *Sci. Rep.* **2020**, *10*, 4966. [CrossRef]
36. Gobinath, R.; Ganapathy, G.P.; Salunkhe, A.A.; Raja, G.; Prasath, E.; Kavya, T. Understanding Soil Erosion Protection Capabilities of Four Different Plants on Silty Soil. In Proceedings of the IOP Conference Series: Materials Science and Engineering, Warangal, India, 9–10 October 2020; Volume 981, p. 032053.
37. Olinic, T.; Olinic, E.D. The effect of living plant roots on the shear strength parameters: A sustainable approach to shallow slope stability and erosion control applications. In Proceedings of the 4th International Conference on Sustainable Development in Civil, Urban and Transportation Engineering, Wroclaw, Poland, 14 October 2024, *in press*.
38. Tang, Y.; Wei, S.; Liu, X.; Liu, W.; Liu, T. Mechanical Analysis of Palm-Fiber-Reinforced Sand through Triaxial Tests. *Sustainability* **2023**, *15*, 5461. [CrossRef]
39. *STAS 9470-73*; Hydrotechnics. Heavy Rainfalls: Intensity-Duration-Frequency Curves. STAS: Bucharest, Romania, 1973.
40. He, Y.; Li, B.; Du, X. Soil slope instability mechanism and treatment measures under rainfall—A case study of a slope in Yunda Road. *Sustainability* **2023**, *15*, 1287. [CrossRef]
41. Artidteang, S.; Tanchaisawat, T.; Bergado, D.T.; Chaiyaput, S. Natural fibers in reinforcement and erosion control applications with limited life geosynthetics. In *Ground Improvement Case Histories: Compaction. Grouting Geosynth*; Butterworth-Heinemann: Oxford, UK, 2015; pp. 717–740.
42. Zhao, L.; Fang, Q.; Hou, R.; Wu, F. Effect of rainfall intensity and duration on soil erosion on slopes with different microrelief patterns. *Geoderma* **2021**, *396*, 115085. [CrossRef]
43. Deng, Y.; Wang, S.; Bai, X.; Luo, G.; Wu, L.; Chen, F.; Wang, J.; Li, C.; Yang, Y.; Hu, Z.; et al. Vegetation greening intensified soil drying in some semi-arid and arid areas of the world. *Agric. For. Meteorol.* **2020**, *292*, 108103. [CrossRef]
44. Foltz, R.B.; Wagenbrenner, N.S. An evaluation of three wood shred blends for post-fire erosion control using indoor simulated rain events on small plots. *Catena* **2010**, *80*, 86–94. [CrossRef]
45. NP 125:2010—Technical Norm: Foundation on Collapsible Soils. Available online: https://www.mdlpa.ro/userfiles/reglementari/Domeniul_III/III_24_NP_125_2010.pdf (accessed on 27 October 2024).

Disclaimer/Publisher's Note: The statements, opinions and data contained in all publications are solely those of the individual author(s) and contributor(s) and not of MDPI and/or the editor(s). MDPI and/or the editor(s) disclaim responsibility for any injury to people or property resulting from any ideas, methods, instructions or products referred to in the content.